40th Thermophysics Conference
23 - 26 June 2008, Seattle, Washington

AIAA 2008-4103

Simulation of FIRE II Reentry Flow Using the Direct Simulation Monte Carlo Method

Erin D. Farbar* and Iain D. Boyd †

Department of Aerospace Engineering, University of Michigan, Ann Arbor, MI 48109

Axisymmetric simulations of hypersonic flow about the FIRE II reentry vehicle using the direct simulation Monte Carlo method are presented. Flow field solutions for points along the FIRE II trajectory in the noncontinuum regime at 85 km altitude, and near continuum regime at 76 km altitude are computed using both an eleven species and a five species chemistry set. The ambipolar diffusion assumption is used to enforce charge neutrality in the flow. The sensitivity of the results for the noncontinuum flow condition are examined with respect to the molecular interaction model for all colliding pairs, and the vibrational relaxation model for collisions of electrons and nitrogen molecules. The results indicate that the degree of ionization of the flow field and the surface heat flux are insensitive to variations in both models. Experimentally and computationally determined total collision cross section data for the interaction of electrons and neutral particles are incorporated into the molecular interaction model. This modification again results in little change to the results for the noncontinuum flow condition. When possible, the simulation results are compared to previous results and to experimental data. The heat flux to the vehicle surface computed using the eleven species chemistry model agrees reasonably well with the data obtained during the FIRE II reentry at the noncontinuum flow condition. In the near continuum regime, the predicted heat flux shows reasonable agreement with the measured data provided the radiative component is included.

Nomenclature

d	diameter in m
g	relative velocity in m/s
k	Boltzmann constant
Kn	Knudsen number
m_r	reduced mass in kg
n	number density in m^{-3}
p	pressure in N/m^2
R_n	radius of capsule forebody
s	surface coordinate in m
T	temperature in K
U	velocity in km/s
α	absorption coefficient
ρ	density in kg/m^3
σ	cross section
ω	parameter in VHS model
ε	energy
ν	collision rate in 1/s
τ	relaxation time in s
ζ	number of degrees of freedom
θ	characteristic temperature in K

*Graduate Student, Student Member AIAA. Email: efarbar@umich.edu
†Professor, Associate Fellow AIAA. Email: iainboyd@umich.edu

Subscripts

e	electron value
r	rotational value
ref	reference value
t	translational value
T	total value
v	vibrational value
wall	wall value
∞	freestream value

I. Introduction

When vehicles reenter the Earth's atmosphere at the super-orbital velocities associated with lunar, Mars or other high energy return trajectories, the resulting particle collisions are sufficiently energetic to produce charged particles through both associative and direct ionization reactions. The resulting weakly ionized plasma surrounding the vehicle affects both the convective and radiative heat transfer to the vehicle surface at these high velocities. The accurate simulation of the flow field composition including charged particles is an important requirement for the computation of radiative heating from the shock layer, which can be a significant portion of the overall heating. It is therefore necessary to incorporate thermochemical models for ionized particle interactions into the DSMC algorithm.

The direct simulation Monte Carlo[1] (DSMC) method has been used extensively to compute neutral rarefied gas flow fields. The Nonequilibrium Gas and Plasma Dynamics research group at the University of Michigan currently uses a state of the art DSMC code called MONACO to simulate neutral rarefied gas flows. The work of the authors is focused on adapting MONACO to include the capability to accurately simulate high energy, weakly ionized flows. The Flight Investigation of Reentry Environment (FIRE) II[2,3] project is used as the baseline flight configuration to test the modifications made to MONACO.

Previous DSMC results have been reported for the FIRE II flow conditions examined in this work. An axisymmetric model of the 76 km flight condition was presented in Ref. 4. This work included models for the electric field created by the movement of the charged particles in the flow, the sheath at the vehicle surface, and radiative heat transfer to the vehicle surface. Reference 4 also presented results obtained using the original models for the incorporation of ionization effects into DSMC, developed by Bird.[5] This method also included a radiation model and resulted in an over prediction of the heat transfer at the capsule surface by about 20%. The same models for the ionization effects presented in Ref. 4 were applied to the 85 km flight condition in Ref. 6, with the exception of the radiation model. The result again over predicted the vehicle heat transfer by 15-20%. In both cases, a finite catalytic coefficient of 0.02 was used for the formation of beryllium oxide at the vehicle surface.

Both the radiation models and the methods for moving the charged particles differ between the two methods discussed above. As this paper does not address the problem of radiation modeling, only the latter is discussed. Bird's method[5] for including the effect of the electric field involves associating an electron with an ion at the time of pair creation and moving them together through out the remainder of the simulation. In the method presented by Taylor et al.,[4] the electric field is calculated by assuming a zero net current and satisfaction of the charge neutrality condition in a given cell, and then averaging over the velocities of particles in that cell to compute the field. The charged particles are then accelerated using this field in the move portion of the DSMC algorithm.

The overall goal of this project is to include the creation and interaction of charged particles in the DSMC method and systematically determine the effect that each portion of the ionization model has on the flow field and on the predicted vehicle surface properties. The results reported here are flow field solutions for both the 76 km and 85 km flight conditions of the FIRE II vehicle, using both 5 species and 11 species chemistry sets and a baseline set of Variable Hard Sphere (VHS) model parameters. The VHS parameters are then varied and cross section data for the interaction of electrons with neutral species are included. The standard correlation for vibrational relaxation time is replaced with the more accurate correlation due to Lee[7] for the collisions of electrons with nitrogen molecules. The effects of these modifications on the flow field and heat transfer to the vehicle surface are examined. The radiative heat transfer to the vehicle is determined from the steady state flow field solution in an uncoupled manner using the NASA NEQAIR code. Lastly, conclusions and suggestions for further work are provided.

II. The FIRE Experiment

Project FIRE was an Apollo era experiment to measure the radiative and convective heating during atmospheric entry at lunar return speeds.[2] The FIRE II reentry vehicle consisted of three phenolic-asbestos heat shields sandwiched between beryllium calorimeters. The first two heat shield and calorimeter packages were designed to be ejected after the onset of melting, yielded heating data free of the effects of ablation and three separate data gathering periods. Calorimeter plugs and radiometers were located at various positions on the heat shields.[2] Both of the flight conditions examined in this study occurred during the first data collection period. Figure 1 is an image of the computational domain showing the grid for the 85 km case and the location of the calorimeter at s/R=0.10 that produced the heat transfer data quoted in this study. The free stream conditions for both the 85 km and 76 km flight conditions are given in Table 1. The freestream Knudsen number is based on the capsule forebody diameter.

III. DSMC Model

Electrons have a mass that is five orders of magnitude lower than that of the heavier air species, and their addition to the flow field necessitates modifications to the DSMC method. If the electrons possess the same translational temperature as the other species, their thermal velocities will be more than two orders of magnitude higher. However, the transport of the electrons will be limited by the electrostatic attraction of the ions and electrons. This phenomenon can be modeled using the assumption of ambipolar diffusion, which requires that ions and electrons move at the same average rate to maintain charge neutrality on scales larger than the Debye length scale. The collision probability in the DSMC algorithm is computed using the product of the collision cross section and the relative velocity of the colliding pair. Due to their high thermal velocities, if one particle of the pair is an electron this rate will be very high, thus requiring a much smaller simulation time step as compared to simulations performed without electrons. Simulations of weakly ionized flow fields thus in general become much more computationally expensive.

In this work, the effect of the electric field is simulated simply by invoking the assumption of ambipolar diffusion and requiring the electrons to move at the average ion velocity in a given cell.[8] Models for rotational[9] and vibrational[10] relaxation during inelastic collisions are included, along with the standard neutral chemistry set and an additional 31 reaction chemistry set involving charged particles and including both associative and direct ionizing reactions.[11] The complete chemistry set is given in Table 2. The reaction rates are implemented within the DSMC framework using the Total Collision Energy (TCE) model, and the Vibrationally-Favored Dissociation (VFD) model[12] is implemented for the dissociation of molecular nitrogen and oxygen utilizing favoring parameters of 2.0 and 0.5, respectively. A baseline set of VHS parameters[1] is used for particle interactions and is given in Table 3. Also given in this table is a modified set of VHS parameters[5] used to explore the sensitivity of the results to the values used in the molecular model. In this work, the properties of the ions are set equal to the properties of the corresponding neutral particles.

The vehicle wall is assumed to be fully catalytic to ions and electrons but not catalytic to atoms or to the formation of BeO as in the earlier work discussed previously. The grid spacing in the direction of flow gradients is less than the local mean free path, and the computational time step is less than the local mean collision time everywhere in the domain. The collision routine is subcycled within each overall simulation time step to accurately simulate collisions of electrons and heavy particles, and the particles are moved with a timestep corresponding to the collision time of heavy particles. Electron-electron collisions are not simulated as these are very frequent and serve solely to thermalize the electron distribution function; it is assumed that collisions of electrons with heavy species are sufficient to do so.

III.A. Calculation of radiative heat flux

The heat flux values obtained from the calorimeters on the FIRE II vehicle include the convective heating as well as a contribution due to the radiation absorbed by the calorimeters, as given in Equation (1). The absorption coefficient for beryllium is a function of wavelength, and is reported to approach 1.0 at wavelengths less than 0.2 μm and decrease at wavelengths greater than 0.2 μm at room temperature.[2] In this work, the radiative heating component is computed in an uncoupled manner using the NEQAIR code[13] by inputting the DSMC flow field. The computed radiative and convective components of the heat flux are then summed to produce a result for the total predicted calorimeter heating rate. In computing the sum given by Equation (1), the absorption coefficient of beryllium is approximated as a constant equal to 1.0 for

wavelengths less than 0.2 μm, and 0.5 for wavelengths greater than 0.2 μm. The error in the predicted total heat flux caused by this approximation is larger at the 76 km flight condition due to the larger contribution of radiative heating to the total heat flux at that altitude.

$$\dot{q}_{measured} = \dot{q}_{convective} + \alpha \dot{q}_{radiative} \tag{1}$$

III.B. Treatment of interactions between electrons and neutral particles

The VHS model that is used to compute the total collision cross section for a colliding pair is formulated to produce a temperature dependence of the macroscopic viscosity coefficient, $\mu \sim T^{\omega+1/2}$, in a gas that is sufficiently close to translational equilibrium that the conditions for the validity of the Chapman-Enskog expansion apply. In the case of collisions of electrons with neutral particles, the relative velocity dependence of the cross sections produced using the standard VHS model with $0 \leq \omega \leq 0.5$ do not agree with the data obtained both experimentally and computationally. In this study, the total cross section data for collisions of electrons with molecular nitrogen, oxygen and atomic nitrogen are fit using the VHS relation given in Equation (2) to produce more accurate model parameters.[14–18] These new parameters are given in Table 4 and are very similar to those presented in Ref. 19. The collision cross section of electrons with molecular nitrogen shows a shape resonance feature in the energy range of 1.5 eV - 4.0 eV. This feature was included in the modeling of e-N_2 collisions as given in Equation (3),[19] where energy (ε) is given in eV. Figures 2, 3 and 4 give the total collision cross sections as a function of relative collision energy for each colliding pair computed with both the baseline and modified VHS parameters, the fits to the data, and the relevant data sets from the literature. In these figures, the correlation due to Bell et al.[20] for the electron impact ionization cross section is given for reference where applicable. From these comparisons it is clear that the addition of more accurate collision cross section data will result in an increased collision rate of the electrons with N, O and N_2, except at collision energies below approximately 1 eV in the case of e-O and e-N_2 collisions. A separate simulation is conducted using the accurate cross section data for one colliding pair at a time, to determine the relative importance of the inclusion of the data for each pair on the results.

$$\sigma_{VHS} = \frac{\sigma_{ref}}{\Gamma(2-\omega)} \left(\frac{2kT_{ref}}{m_r} \right)^{\omega} g^{-2\omega} \tag{2}$$

$$\begin{aligned} \sigma_T &= \sigma_{VHS} + \frac{22}{0.7} (\varepsilon - 1.5), 1.5 \leq \varepsilon \leq 2.2, \mathring{A}^2 \\ \sigma_T &= \sigma_{VHS} - \frac{22}{1.8} (\varepsilon - 4.0), 2.2 < \varepsilon \leq 4.0, \mathring{A}^2 \end{aligned} \tag{3}$$

III.C. Electron impact vibrational relaxation of nitrogen

The baseline solutions for both flight conditions are obtained using the Millikan and White correlation for vibrational relaxation time of various colliding species pairs[21] with a high temperature correction due to Park.[22] The 85 km case is also computed using the correlation for e - N_2 vibrational relaxation time due to Lee.[7] The correlation is implemented as shown in Equation (4). The averaged product, $\overline{\sigma_T g}$, is evaluated at each time step in each cell using an average translational temperature and the VHS expression for the given cell. The correction factor for conversion of the continuum collision number to a collision number applicable to particle simulations is due to Lumpkin et al.[23] The number of vibrational degrees of freedom is approximated as a constant throughout the simulation, and is calculated using Equation (5) and a reference temperature of 10 000 K.

$$\begin{aligned} P_{Lee,vib.} &= factor \times \frac{1}{\nu \tau_{e-V}} \\ \nu \tau_{e-V} &= n_{N_2} \overline{\sigma_T g} \frac{(p_e \tau_{e-v})_{Lee}}{n_e k T_e} \\ factor &= \frac{\zeta_t + \zeta_v}{\zeta_t} \end{aligned} \tag{4}$$

$$\zeta_v = \frac{2\theta_v/T_{ref}}{e^{\theta_v/T_{ref}} - 1} \tag{5}$$

IV. Results and Discussion

A general impression of the flow field surrounding the FIRE II vehicle at the 85 km flight condition is given in Fig. 5, where contours of the translational temperature are shown. Figure 6 shows the temperatures of the rotational, vibrational, translational and electron translational modes along the stagnation streamline for the 85 km flight condition obtained using both the 5 species and 11 species chemistry models. The addition of ionization chemistry to the model narrows the translational temperature profile. The peak translational temperature is approximately 52 000 K, and the rotational temperature is decreased significantly in the 11 species case as compared to the 5 species case. This is likely due to an increased level of dissociation in the 11 species simulation. These trends were also observed in computations of this FIRE II flight condition reported in Ref. 6, however the temperature shock stand off distance obtained here appears to be slightly larger than that presented in Ref. 6. This issue is addressed in the following subsection. Figures 7 and 8 give the mole fractions of the neutral and charged species along the stagnation line. The electron mole fraction peaks at a value of approximately 0.02, again in agreement with the results presented in Ref. 6. Figure 9 shows the number density of electrons, total number density of ions, and the degree of ionization along the stagnation line. Charge neutrality is reasonably enforced in the flow field and the degree of ionization peaks at approximately 2% downstream of the shock.

Figure 10 shows the heat flux profiles at the capsule surface for both the 11 species and 5 species simulations, along with a measured data point.[2] The reported error on the measured data was ±5%. The simulation incorporating ionization effects yields a slightly lower convective heat flux than the neutral gas simulation. It is likely that this is due to an increased amount of dissociated nitrogen. While the ionization reactions result in a slight increase in the number density of the flow, it is likely that the main reason for this increase in nitrogen dissociation is due to the inclusion of the mechanism of electron impact dissociation, Reaction 1E in Table 2. This rate is two orders of magnitude higher than the rates for dissociation of nitrogen due to collisions with atoms and molecules. This hypothesis is supported by the profiles of mole fraction shown along the stagnation streamline in Fig. 7, where it is evident that there is a larger fraction of atomic nitrogen and a smaller fraction of molecular nitrogen downstream of the shock in the 11 species simulation. The net effect is that the temperature profiles are more shallow at the capsule surface in the 11 species simulation than in the 5 species simulation. It should be noted that the results of Taylor et al.[6] indicated that the addition of ionization chemistry resulted in a net increase of the capsule heat transfer. However, it is likely that the finite catalycity of the wall to oxygen atoms in that simulation negated the effect described here. The convective heating results obtained using the 11 species chemistry set fall at the top of the error bar range of the FIRE II data. The computed radiative heat flux is 7.5 W/cm^2 along the line of sight indicated in Fig. 1. A data point representing the summation of the computed radiative and convective heat flux is shown on Fig. 10. Taylor et al.[6] reported results that overpredicted the total heat transfer by 30% in the stagnation region at this flight condition; these results are also shown in Fig. 10. The contribution of absorbed radiation to the measured heat flux at this flight condition is small.

The temperature profiles along the stagnation streamline for the 76 km flight condition are shown in Fig. 11 for both the 11 species and 5 species chemistry models. In this case, the addition of ionization has a much more pronounced effect on the flow field, causing a relatively large movement of the shock towards the vehicle surface. The peak translational temperature is approximately 53 000 K, and the rotational temperature is significantly reduced in the 11 species case. These trends are also reported in Ref. 4, however again the shock standoff distance reported in Ref. 4 is slightly smaller than that shown in Fig. 11. There is more scatter present in the data for both T_v and T_r produced using the 5 species chemistry model because the exclusion of ionization chemistry results in a lower number density of molecular species in the flow field. Figure 12 shows the mole fractions of the charged species along the stagnation line. In this case the electron mole fraction peaks at approximately 0.07. The most abundant ion in the flow field is N^+ with a peak mole fraction of 0.05. Both of these results are in agreement with data obtained using Bird's method[5] in Ref. 4. The number density of electrons and ions, and the degree of ionization along the stagnation streamline are presented in Fig. 13. Again, charge neutrality is enforced in the flow field. The degree of ionization peaks at approximately 7% downstream of the shock in this case.

Figure 14 shows the computed heat flux at the capsule surface for both chemistry sets along with the

measured data point for the 1634 second flight condition. The 11 species simulation underpredicts the measured heat transfer by approximately 20% without the radiative component included. The radiative component of the heat flux was found to be 28.6 W/cm^2 at this altitude. A data point representing the summation of the computed radiative and convective heat flux is shown in Fig. 14. The DSMC result including the radiative heating component slightly underpredicts the measured heat transfer at this flight condition. Taylor et al.[4] reported results that overpredicted the total heat transfer by 20%-30% in the stagnation region at this flight condition; these results are also shown in Fig. 14. In the simulations presented here, the wall is catalytic only to charged species.

IV.A. Sensitivity to VHS parameters

The 85 km case is simulated using the modified VHS parameters listed in Table 3 in order to determine the sensitivity of the flow field results of interest to the VHS parameters used in the calculation. Figure 15 shows the temperature profiles along the stagnation streamline for each VHS data set. The modified VHS parameters give slightly higher peak rotational and translational temperatures, and a shorter temperature shock stand off distance than the baseline parameters. These results are consistent as a decrease in the VHS parameter, ω, results in an increase in the cross section computed using the VHS model at a given collision energy, and thus a decrease in the rate of energy transport in the flow. However, there is no appreciable change in the overall degree of ionization of the flow field, the convective heat transfer to the capsule surface, nor the radiative heat transfer computed using NEQAIR. The temperature shock stand off distance seen in Fig. 15 agrees more closely with the results represented in Ref. 6 but is still slightly larger. It is likely that the VHS model parameters employed in Ref. 4 and Ref. 6 were those given in Ref. 5, which correspond to the modified parameter set presented here.

IV.B. Sensitivity to electron-neutral total cross section

Three simulations at the 85 km flight condition are conducted in which the VHS parameters for electron collisions with nitrogen molecules and atoms, and oxygen atoms from the modified model are replaced with the more accurate parameters obtained by fitting the measured and calculated data. No appreciable change is observed in the temperature profiles along the stagnation line, nor in the heat transfer to the vehicle surface. It should be noted that the total collision cross section is used in computing the instantaneous reaction probability for a colliding pair within the framework of the TCE and VFD chemistry models. Thus, increasing the collision cross section for collisions of electrons and neutral species does not also increase the frequency with which the associated chemical reactions occur.

IV.C. Sensitivity to vibrational relaxation model

A simulation at the 85 km flight condition is conducted using the Lee[7] correlation for the vibrational relaxation time of nitrogen molecules colliding with electrons. The temperatures obtained using this model are plotted along the stagnation streamline in Fig. 16. For a given set of flow conditions, the relaxation probability computed using the vibrational relaxation model[10] with the Millikan and White data is higher than that computed using the Lee correlation, except at temperatures in the vicinity of the minimum value of the relaxation coefficient. This minimum occurs at approximately 7 000 K. Thus, the use of the correlation due to Lee rather than that due to Millikan and White causes a slightly larger separation of the vibrational and electron translational temperatures in the post shock region. However, the temperature differences have a negligible effect on the heat flux to the capsule surface, as the vibrational and electron translational temperatures equilibrate upstream of the capsule surface.

V. Conclusions and Future Work

The flow field results obtained for both the 85 km and 76 km flight conditions for the FIRE II reentry vehicle agree qualitatively with the previously published data. Specifically, the peak values of translational temperature, electron mole fraction, and major ion species mole fractions agree quantitatively with data obtained using the method of Bird at the 76 km condition, and that of Taylor et al. at the 85 km condition, where those data are available. The temperature shock stand off distance computed using the baseline VHS

parameters is slightly larger than that reported using Bird's method, however it is shown that the variation of the VHS parameters results in a notable decrease in this distance.

The computed result for the total heat transfer at the capsule surface slightly overpredicts the experimental data at the 85 km flight condition. At the 76 km flight condition, the computed total heat transfer slightly underpredicts the data.

The variation of the VHS model parameters has a noticeable effect on the computed temperature shock stand off distance. Use of the Lee correlation to compute the vibrational relaxation time for nitrogen molecules colliding with electrons results in an increased equilibration time of the vibrational and electron translational temperatures, however the effect of this change on the heat flux to the capsule surface and degree of ionization in the flow field is negligible. The addition of accurate total collision cross section data for collisions of electrons with neutral particles has no visible effect on the flow field solution.

The model of charged particle interaction used in this work fails to model the acceleration of charged particles due to the electric field that is generated in the shock region. Additionally, although accurate collision cross section data have been implemented for electron - neutral collisions, the important electron impact ionization and associative ionization reactions are currently implemented with the TCE model. It is desirable to improve both of these areas, and quantify the effects on the solution parameters of interest for a high energy reentry trajectory.

Acknowledgments

The authors gratefully acknowledge the financial support provided by NASA grant NCC3-989.

References

[1]Bird, G. A., "Monte Carlo Simulation in an Engineering Context," *Rarefied Gas Dynamics*, edited by S. S. Fisher, Vol. 74 of *Progress in Astronautics and Aeronautics*, AIAA, New York, 1981, pp. 239–255.

[2]Cornette, E. S., "Forebody Temperatures and Calorimeter Heating Rates Measured During Project Fire II Reentry at 11.35 Kilometers Per Second," Tech. Rep. NASA TM X-1305, Langley Research Center, 1966.

[3]Cauchon, D. L., McKee, C. W., and Cornette, E. S., "Radiative Heating Results from the Fire II Flight Experiment at a Reentry Velocity of 11.4 Kilometers per Second," Tech. Rep. NASA TM X-1402, Langley Research Center, 1967.

[4]Taylor, J. C., Carlson, A. B., and Hassan, H. A., "Monte Carlo Simulation of Radiating Re-entry Flows," *Journal of Thermophysics and Heat Transfer*, Vol. 8, No. 3, 1994, pp. 478–485.

[5]Bird, G. A., "Nonequilibrium Radiation During Re-entry at 10 km/s." *AIAA 22nd Thermophysics Conference*, 1987, AIAA-87-1543.

[6]Taylor, J. C., Carlson, A. B., and Hassan, H. A., "Monte Carlo Simulation of Reentry Flows with Ionization," *30th AIAA Aerospace Sciences Meeting and Exhibit*, 1992, AIAA-1992-0493.

[7]Lee, J.-H., "Electron-impact Vibrational Relaxation in High-temperature Nitrogen." *Journal of Thermophysics and Heat Transfer*, Vol. 7, No. 3, 1993, pp. 399–405.

[8]Boyd, I. D., "Monte Carlo Simluation of Nonequilibrium Flow in a Low-power Hydrogen Arcjet," *Physics of Fluids*, Vol. 9, No. 10, 1997, pp. 4575–4584.

[9]Boyd, I. D., "Rotational-translational Energy Transfer in Rarefied Nonequilibrium Flows," *Physics of Fluids*, Vol. 2, No. 3, 1989, pp. 447–452.

[10]Boyd, I. D., "Analysis of Vibrational-translational Energy Transfer Using the Direct Simulation Monte Carlo Method," *Physics of Fluids*, Vol. 3, No. 7, 1991, pp. 1785–1791.

[11]Boyd, I. D., Trumble, K., and Wright, M. J., "Nonequilibrium Particle and Continuum Analyses of Stardust Entry for Near-Continuum Conditions," *38th AIAA Aerospace Sciences Meeting and Exhibit*, 2007, AIAA-2007-4543.

[12]Haas, B. L. and Boyd, I. D., "Models for Direct Monte Carlo Simulation of Coupled Vibration-Dissociation," *Physics of Fluids*, Vol. 5, No. 2, 1993, pp. 478–489.

[13]Whiting, E., Park, C., Liu, Y., Arnold, J. O., and Paterson, J. A., "NEQAIR96, Nonequilibrium and Equilibrium Radiative Transport and Spectra Program: User's Manual," Tech. Rep. NASA RP-1389, 1996.

[14]Itikawa, Y., "Cross Sections for Electron Collisions with Nitrogen Molecules," *Journal of Physical Chemistry Reference Data*, Vol. 35, No. 1, 2006, pp. 31–53.

[15]Itikawa, Y. and Ichimura, A., "Cross Sections for Collisions of Electrons and Photons with Atomic Oxygen," *Journal of Physical Chemistry Reference Data*, Vol. 19, No. 3, 1990, pp. 637–651.

[16]Sunshine, G., Aubrey, B. B., and Bederson, B., "Absolute Measurements of Total Cross Sections for the Scattering of Low-Energy Electrons by Atomic and Molecular Oxygen," *Physical Review*, Vol. 154, No. 1, 1967, pp. 1–8.

[17]Thomas, L. D. and Nesbet, R. K., "Low-energy Electron Scattering by Atomic Nitrogen," *Physical Review A*, Vol. 12, No. 6, 1975, pp. 2369–2377.

[18]Blaha, M. and Davis, J., "Elastic Scattering of Electrons by Oxygen and Nitrogen at Intermediate Energies," *Physical Review A*, Vol. 12, No. 6, 1975, pp. 2319–2324.

[19]Ozawa, T., Nompelis, I., Levin, D. A., Barnhardt, M., and Candler, G. V., "DSMC-CFD Comparison of a High Altitude, Extreme-Mach Number Reentry Flow," *46th AIAA Aerospace Sciences Meeting and Exhibit*, 2008, AIAA-2008-1216.

[20]Bell, K. L., Gilbody, H. B., Hughes, J. G., Kingston, A. E., and Smith, F. J., "Recommended Data on the Electron Impact Ionization of Light Atoms and Ions," *Journal of Physical and Chemical Reference Data*, Vol. 12, No. 4, 1983, pp. 891–917.

[21]Millikan, R. C. and White, D. R., "Systematics of Vibrational Relaxation," *Journal of Chemical Physics*, Vol. 39, No. 12, 1963, pp. 3209–3213.

[22]Park, C., "Problems of Rate Chemistry in the Flight Regimes of Aeroassisted Orbital Transfer Vehicles," *19th AIAA Thermophysics Conference*, 1984, AIAA-84-1730.

[23]Lumpkin, F. E., Haas, B. L., and Boyd, I. D., "Resolution of Differences Between Collision Number Definitions in Particle and Continuum Simulations," *Physics of Fluids A*, Vol. 3, No. 9, 1991, pp. 2282–2284.

Table 1: Flow conditions for Project FIRE II at 1631 s and 1634 s.

Property	1631 s	1634 s
Altitude	84.6 km	76.4 km
ρ_∞	9.15×10^{-6}kg/m^3	3.72×10^{-5}kg/m^3
U_∞	11.37 km/s	11.36 km/s
T_∞	212 K	195 K
T_{wall}	460 K	615 K
R_n	0.9347 m	0.9347 m
Kn_∞	0.01	0.003

Table 2: Reaction rate coefficients in m^3/molecule/s.

Number	Reaction	Rate Coefficient
1M	$N_2 + M \rightarrow N + N + M$	$1.162\times10^{-8}T^{-1.6}\exp(-113\ 200/T)$
1MB	$N + N + M \rightarrow N_2 + M$	$5.691\times10^{-40}T^{-1.6}$
1A	$N_2 + A \rightarrow N + N + A$	$4.980\times10^{-8}T^{-1.6}\exp(-113\ 200/T)$
1AB	$N + N + A \rightarrow N_2 + A$	$1.706\times10^{-39}T^{-1.6}$
1E	$N_2 + E^- \rightarrow N + N + E^-$	$4.980\times10^{-6}T^{-1.6}\exp(-113\ 200/T)$
2M	$O_2 + M \rightarrow O + O + M$	$3.321\times10^{-9}T^{-1.5}\exp(-59\ 400/T)$
2MB	$O + O + M \rightarrow O_2 + M$	$6.305\times10^{-44}T^{-0.5}$
2A	$O_2 + A \rightarrow O + O + A$	$1.660\times10^{-8}T^{-1.5}\exp(-59\ 400/T)$
2AB	$O + O + A \rightarrow O_2 + A$	$1.905\times10^{-43}T^{-0.5}$
3M	$NO + M \rightarrow N + O + M$	$8.302\times10^{-15}\exp(-75\ 500/T)$
3MB	$N + O + M \rightarrow NO + M$	$1.583\times10^{-43}T^{-0.5}$
3A	$NO + A \rightarrow N + O + A$	$1.826\times10^{-13}\exp(-75\ 500/T)$
3AB	$N + O + A \rightarrow NO + A$	$3.180\times10^{-43}T^{-0.5}$
4F	$O + NO \rightarrow N + O_2$	$1.389\times10^{-17}\exp(-19\ 700/T)$
4B	$N + O_2 \rightarrow O + NO$	$4.601\times10^{-15}T^{-0.546}$
5F	$O + N_2 \rightarrow N + NO$	$1.069\times10^{-12}T^{-1.000}\exp(-37\ 500/T)$
5B	$N + NO \rightarrow O + N_2$	$4.059\times10^{-12}T^{-1.359}$
6F	$N + N \rightarrow N_2^+ + E^-$	$3.387\times10^{-17}\exp(-67\ 700/T)$
6B	$N_2^+ + E^- \rightarrow N + N$	$7.274\times10^{-12}T^{-0.650}$
7F	$O + O \rightarrow O_2^+ + E^-$	$1.859\times10^{-17}\exp(-81\ 200/T)$
7B	$O_2^+ + E^- \rightarrow O + O$	$1.453\times10^{-4}T^{-2.412}$
8F	$N + O \rightarrow NO^+ + E^-$	$8.766\times10^{-18}\exp(-32\ 000/T)$
8B	$NO^+ + E^- \rightarrow N + O$	$1.321\times10^{-9}T^{-1.187}$
9	$N + E^- \rightarrow N^+ + 2E^-$	$8.434\times10^{-14}\exp(-121\ 000/T)$
10	$O + E^- \rightarrow O^+ + 2E^-$	$1.054\times10^{-14}\exp(-106\ 200/T)$
11F	$N_2 + O^+ \rightarrow O + N_2^+$	$1.511\times10^{-18}T^{0.360}\exp(-22\ 800/T)$
11B	$O + N_2^+ \rightarrow N_2 + O^+$	$1.978\times10^{-18}T^{0.109}$
12F	$NO + O^+ \rightarrow O_2 + N^+$	$2.324\times10^{-25}T^{1.900}\exp(-15\ 300/T)$
12B	$O_2 + N^+ \rightarrow NO + O^+$	$2.443\times10^{-26}T^{2.102}$
13F	$O_2 + NO^+ \rightarrow NO + O_2^+$	$3.985\times10^{-17}T^{0.410}\exp(-32\ 600/T)$
13B	$NO + O_2^+ \rightarrow O_2 + NO^+$	$6.195\times10^{-16}T^{-0.050}$
14F	$N + NO^+ \rightarrow O + N_2^+$	$1.195\times10^{-16}\exp(-35\ 500/T)$
14B	$O + N_2^+ \rightarrow N + NO^+$	$1.744\times10^{-18}T^{0.302}$
15F	$O + NO^+ \rightarrow O_2 + N^+$	$1.660\times10^{-18}T^{0.500}\exp(-77\ 2000/T)$
15B	$O_2 + N^+ \rightarrow O + NO^+$	$2.192\times10^{-17}T^{0.114}$
16F	$N + O_2^+ \rightarrow O_2 + N^+$	$1.444\times10^{-16}T^{0.140}\exp(-28\ 600/T)$
16B	$O_2 + N^+ \rightarrow N + O_2^+$	$4.993\times10^{-18}T^{-0.004}$
17F	$N_2 + O_2^+ \rightarrow O_2 + N_2^+$	$1.644\times10^{-17}\exp(-40\ 700/T)$
17B	$O_2 + N_2^+ \rightarrow N_2 + O_2^+$	$4.589\times10^{-18}T^{-0.037}$
18F	$N + NO^+ \rightarrow N_2 + O^+$	$5.645\times10^{-17}T^{-1.080}\exp(-12\ 800/T)$
18B	$N_2 + O^+ \rightarrow N + NO^+$	$3.970\times10^{-18}T^{-0.710}$
19F	$O + NO^+ \rightarrow N + O_2^+$	$1.195\times10^{-17}T^{0.290}\exp(-48\ 600/T)$
19B	$N + O_2^+ \rightarrow O + NO^+$	$8.918\times10^{-13}T^{-0.969}$
20F	$O + O_2^+ \rightarrow O_2 + O^+$	$6.641\times10^{-18}T^{-0.09}\exp(-18\ 600/T)$
20B	$O_2 + O^+ \rightarrow O + O_2^+$	$4.993\times10^{-18}T^{-0.004}$
21F	$N_2 + N^+ \rightarrow N + N_2^+$	$1.660\times10^{-18}T^{0.500}\exp(-12\ 100/T)$
21B	$N + N_2^+ \rightarrow N_2 + N^+$	$2.343\times10^{-14}T^{-0.610}$

Table 3: Parameters used in the VHS model.

Parameter	Baseline value	Modified value
ω	0.25	0.20
T_{ref}	273 K	288 K
d_{N_2}	4.17×10^{-10} m	4.07×10^{-10} m
d_{O_2}	4.07×10^{-10} m	3.96×10^{-10} m
d_{NO}	4.20×10^{-10} m	4.00×10^{-10} m
d_N	3.60×10^{-10} m	3.00×10^{-10} m
d_O	3.10×10^{-10} m	3.00×10^{-10} m

Table 4: Parameters used in the VHS model for collisions of electrons with neutral species.

Colliding pair	σ_{ref}	T_{ref}	ω
N_2 - e	$7.0\times10^{-20}m^2$	288 K	-0.10
N - e	$2.7\times10^{-19}m^2$	288 K	0.19
O - e	$6.0\times10^{-20}m^2$	288 K	-0.05

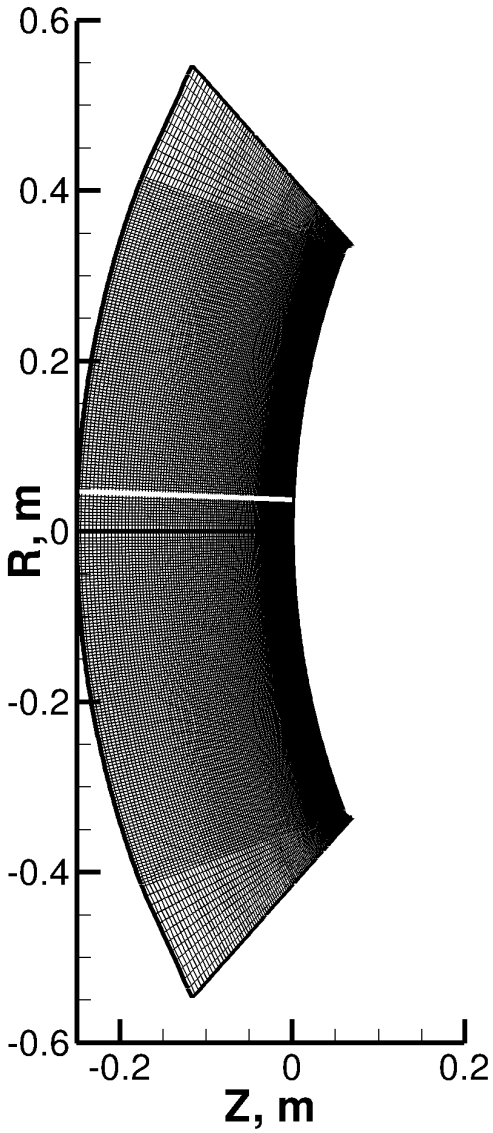

Figure 1: Computational domain and grid for the 85 km case. White line originates from the location of the forebody calorimeter on the vehicle surface, from which the data is quoted for this study. It also indicates the line of sight used for radiation calculations.

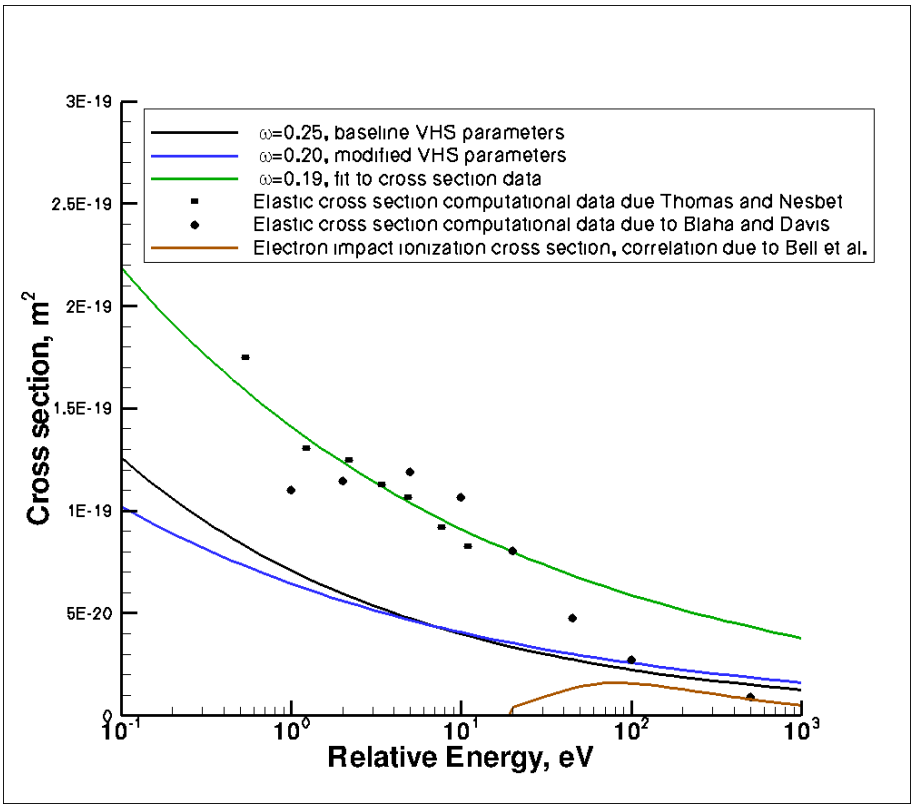

Figure 2: Total collision cross section, e-N collisions.

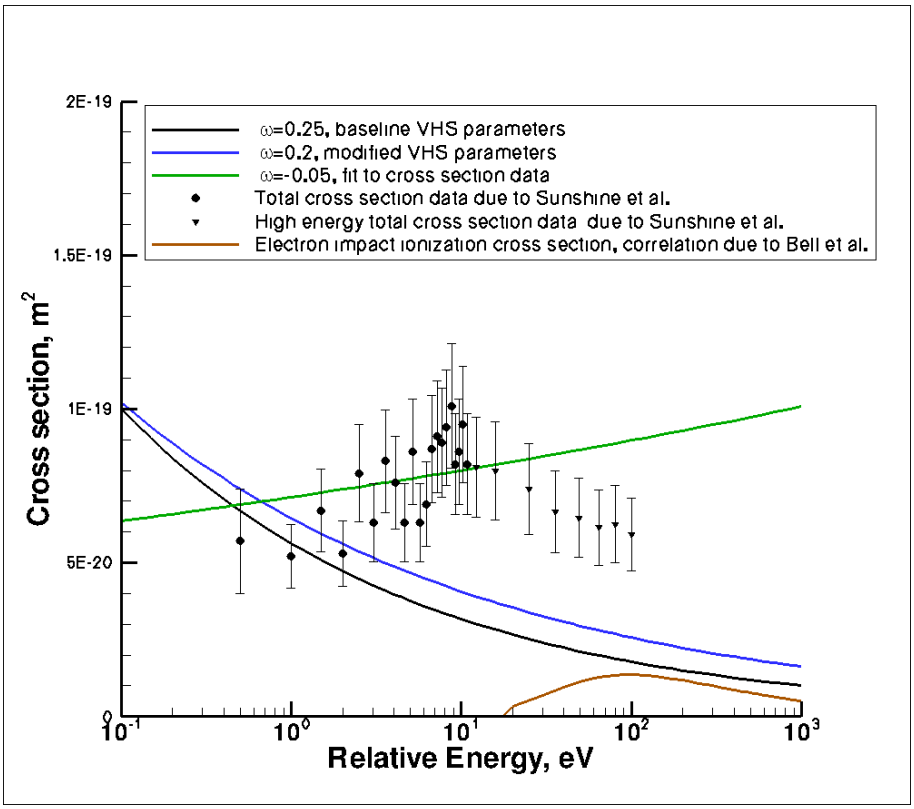

Figure 3: Total collision cross section, e-O collisions.

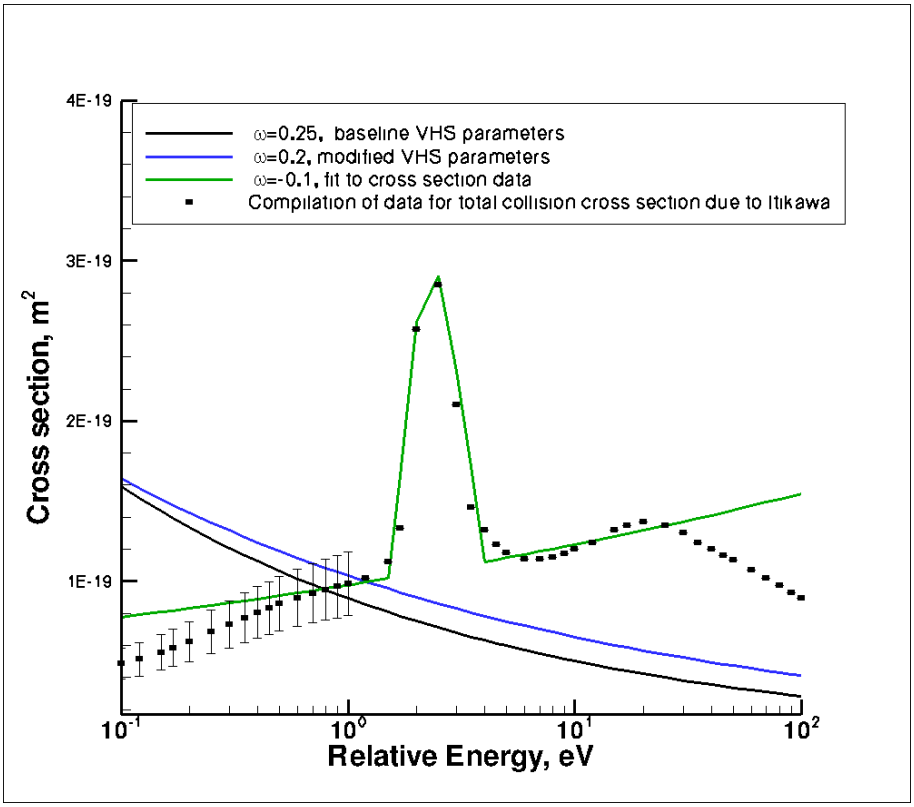

Figure 4: Total collision cross section, e-N_2 collisions.

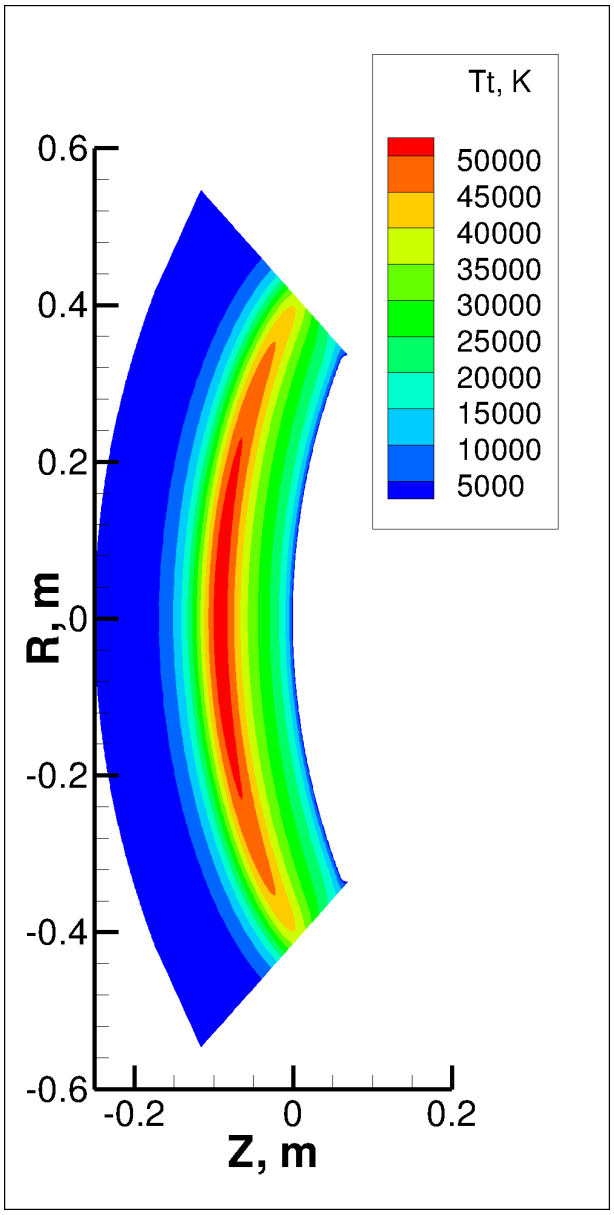

Figure 5: Contours of translational temperature for the 11 species, 85 km case.

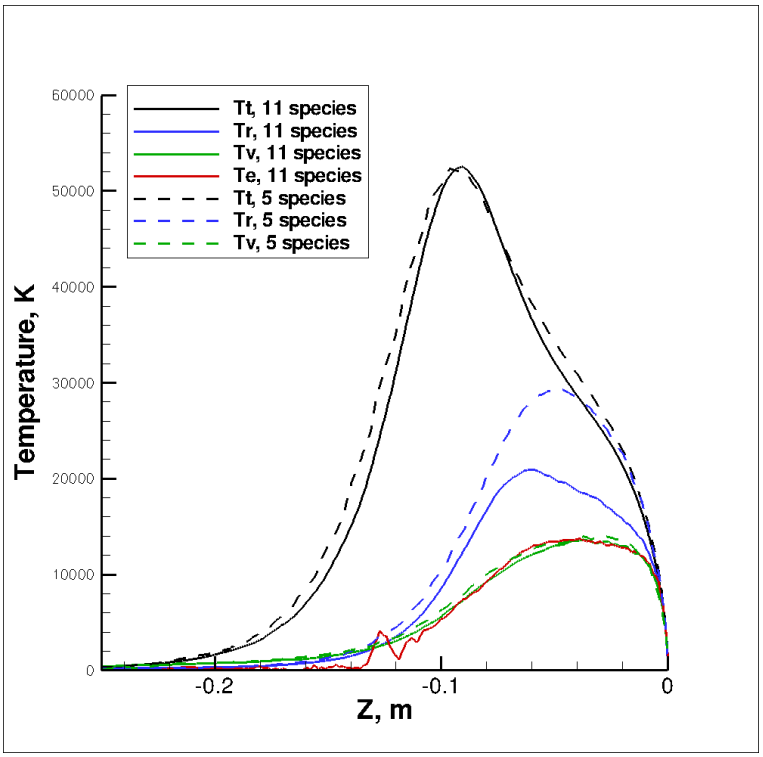

Figure 6: Temperatures along the stagnation streamline for both the 11 species and 5 species chemistry sets, 85 km case.

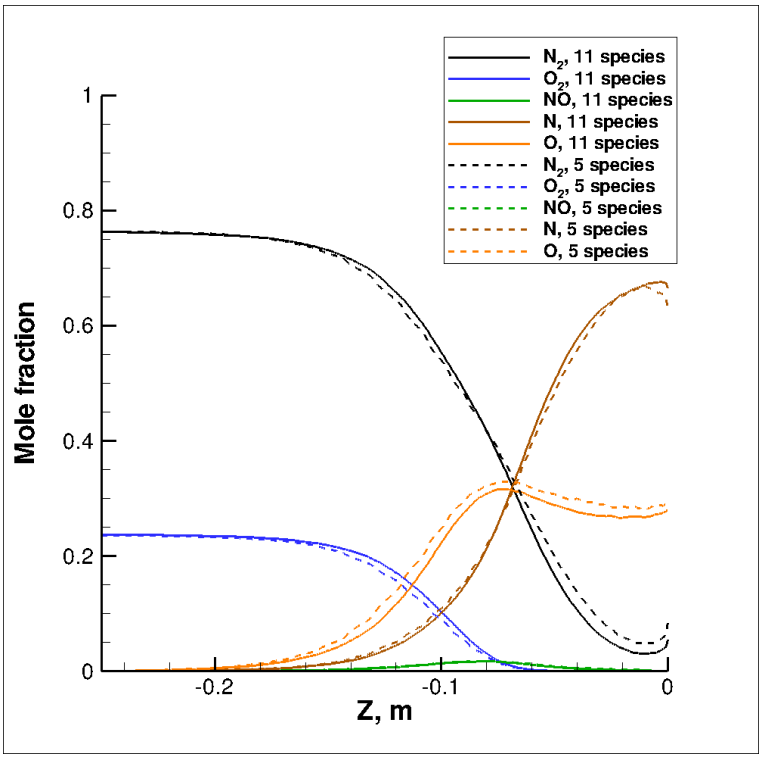

Figure 7: Mole fractions of neutral species along the stagnation streamline for both the 11 species and 5 species chemistry sets, 85 km case.

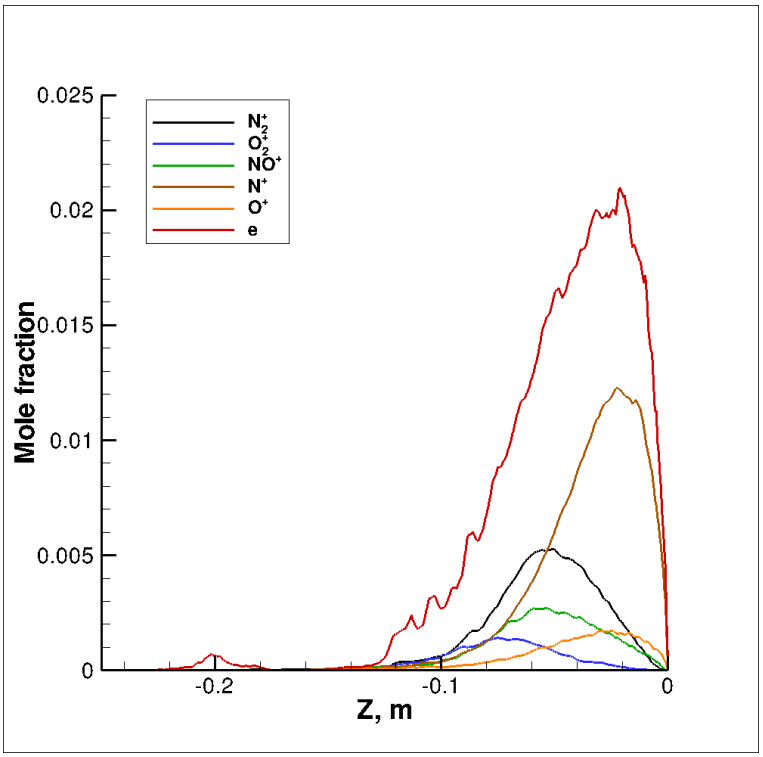

Figure 8: Mole fractions of charged species along the stagnation streamline, 85 km case.

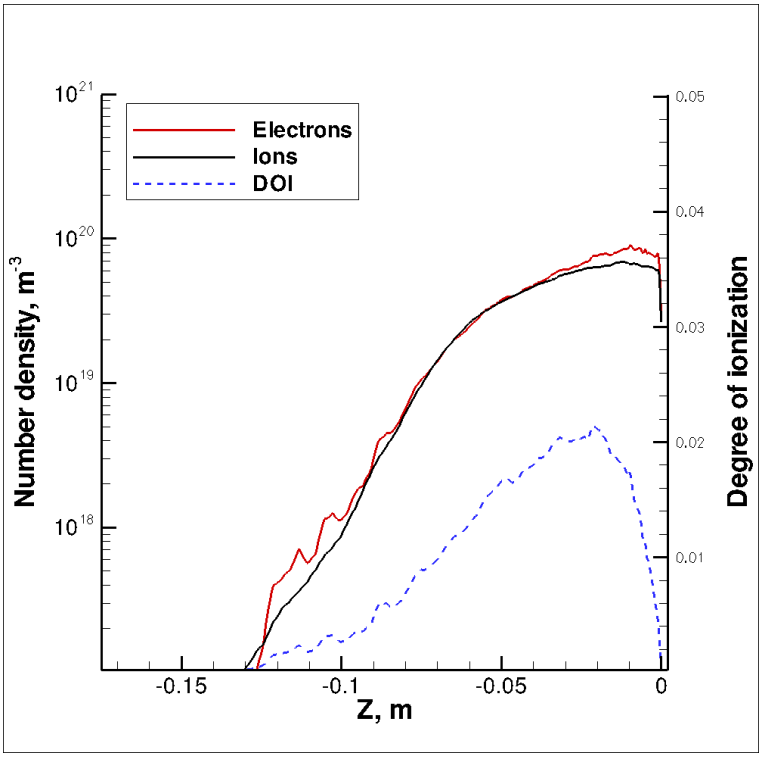

Figure 9: Number density of electrons and ions and degree of ionization along the stagnation streamline, 85 km case.

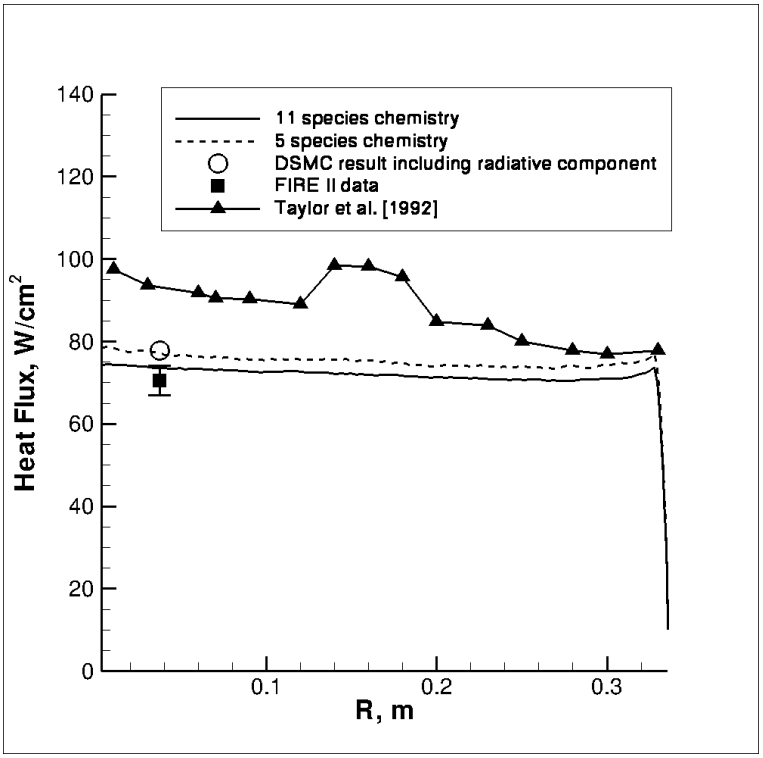

Figure 10: Heat transfer at the capsule surface for both the 11 species and 5 species chemistry sets, 85 km case. Square data point is the measured heat transfer from the FIRE II experiment. Circular data point is the DSMC result including the radiative component. Triangular points are data due to Taylor et al.[6]

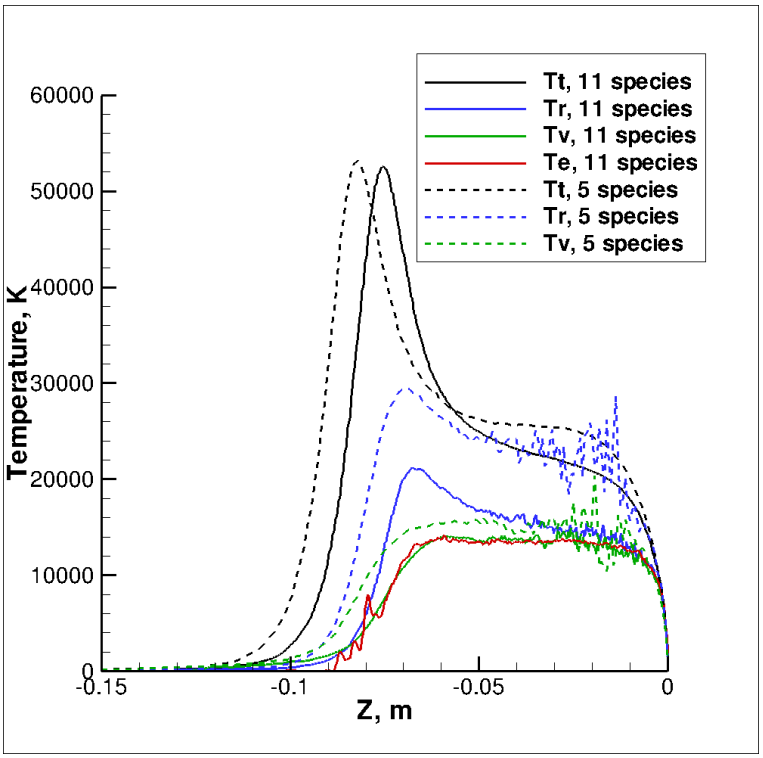

Figure 11: Temperatures along the stagnation streamline for both the 11 species and 5 species chemistry sets, 76 km case.

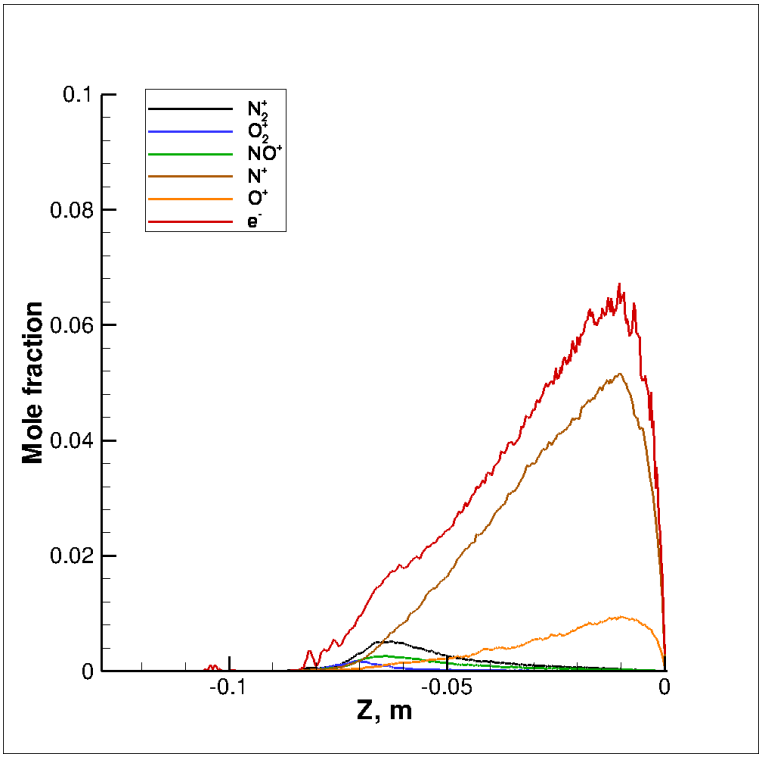

Figure 12: Mole fractions of charged species along the stagnation streamline, 76 km case.

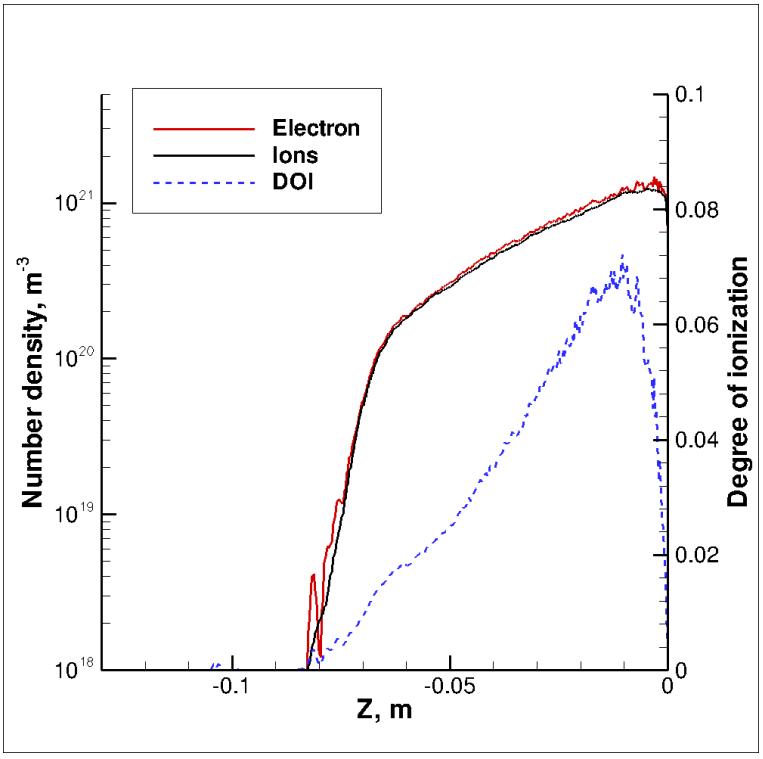

Figure 13: Number density of electrons and ions and degree of ionization along the stagnation streamline, 76 km case.

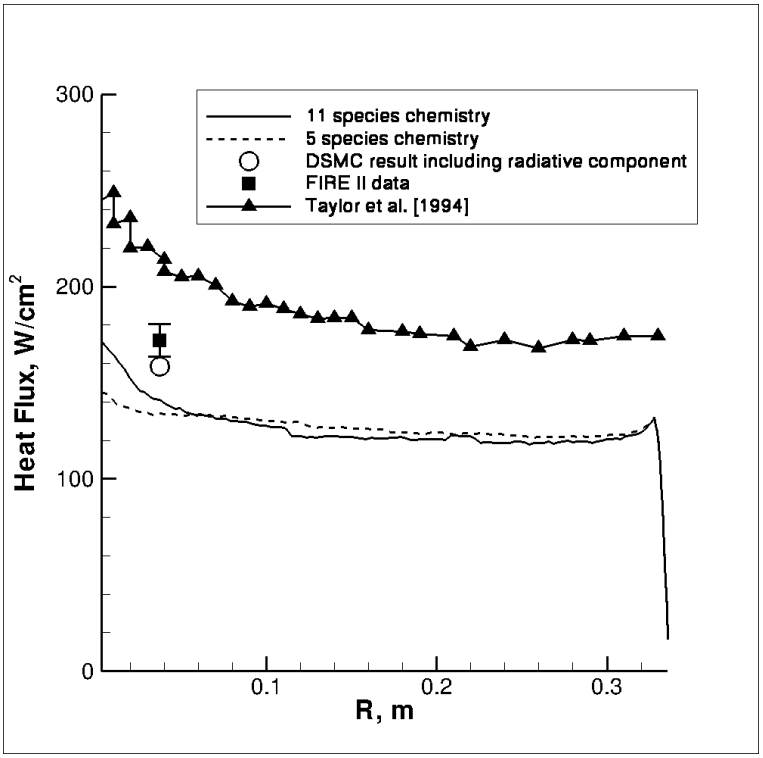

Figure 14: Heat transfer at capsule surface for both the 11 species and 5 species chemistry sets, 76 km case. Square data point is the measured heat transfer from the FIRE II experiment. Circular data point is the DSMC result including the radiative component. Triangular points are data due to Taylor et al.[4]

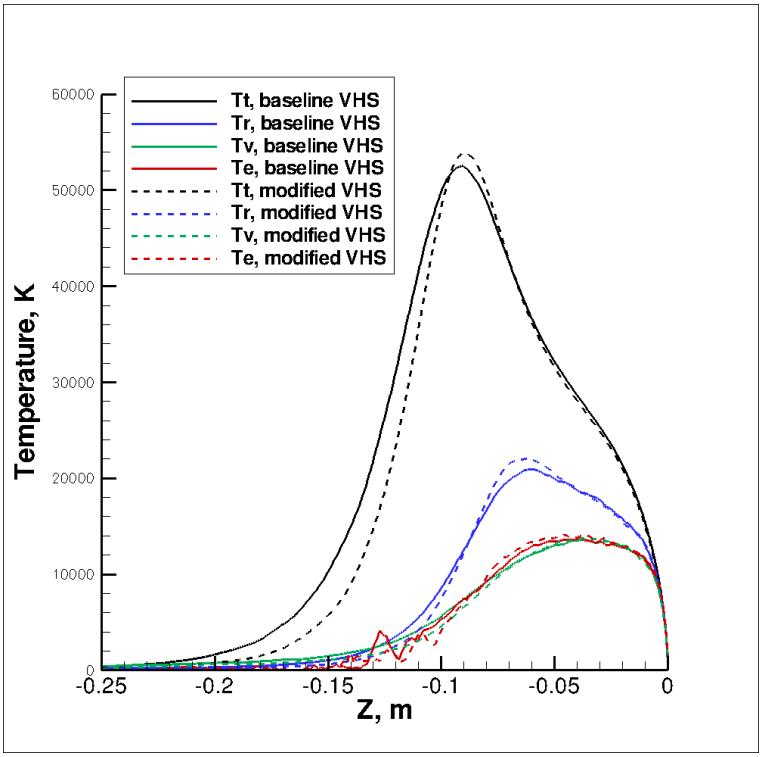

Figure 15: Temperatures along the stagnation streamline for both the baseline and modified VHS models, 11 species, 85 km case.

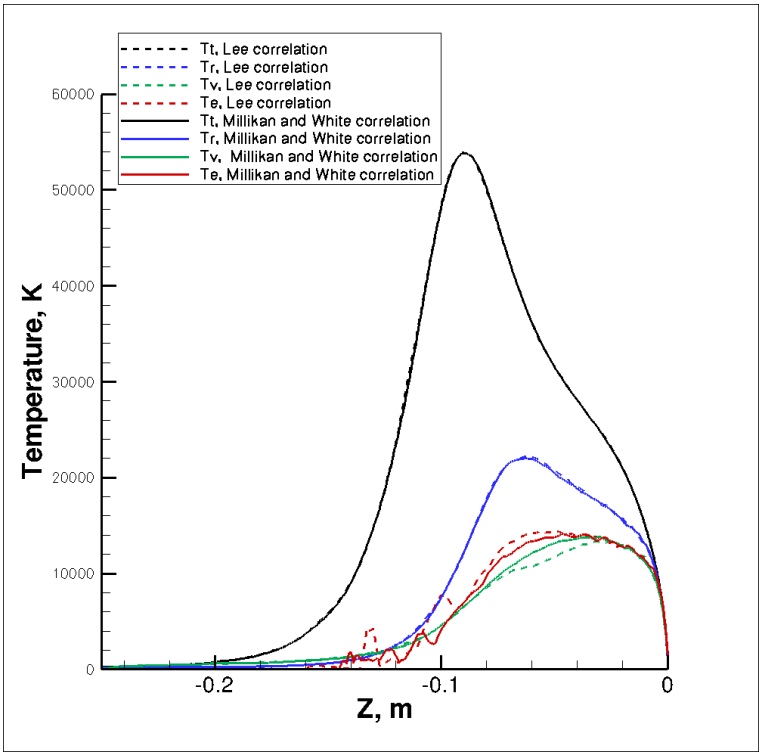

Figure 16: Temperatures along the stagnation streamline for the 85 km case, illustrating the effect of employing the Lee correlation for electron impact vibrational relaxation of nitrogen molecules.